

Search for SM Higgs via $gg \rightarrow h \rightarrow W^*W^*$
with $W^*W^* \rightarrow l\nu$ jet jet
at the TeVatron Run II

Arnaud Lucotte

University of New York at Stony Brook

Abstract

A search for a SM Higgs produced via the gluon-gluon fusion is presented. We investigate here the decay channel $gg \rightarrow h \rightarrow WW^*$ with WW^* where $W^*W^* \rightarrow l\nu$ jet jet. Theoretical calculations establish the corresponding cross-section to be about 100 fb for higgs mass around the WW threshold. In this range mass, di-boson decays are dominant whereas the $b\bar{b}$ channel dominates the Higgs decays below 140 GeV/c².

The selection of a signal in the $W^*W^* \rightarrow l\nu$ jet jet channel faces huge level of backgrounds, as expected in a $p\bar{p}$ collider. The main background comes from the single W production associated with two or more QCD jets: W q/g $\rightarrow l\nu$ jet jet. Other backgrounds come from the di-boson productions $WW \rightarrow l\nu$ jet jet and $WZ \rightarrow l\nu$ jet jet, which mimic the signal topology, as well as from the $t\bar{t}$ events decaying in $t\bar{t} \rightarrow b\bar{b} l \nu$ jet jet.

In our analysis, we use a set of pre-selection cuts to isolate a clean and central signal while rejecting the (soft) QCD jets background. We then define a likelihood function to discriminate signal events from backgrounds on the basis of topology differences. Preliminary Monte Carlo studies show that a 3σ significance effect needs an integrated luminosity of 150 fb⁻¹, whereas a 95% CL exclusion requires a luminosity of about 60 fb⁻¹, for a 160 GeV/c² Higgs. We conclude that this channel has to be used in combination with the associated Higgs production channel.

to be printed in color

Contents

1	Cross-sections and physics Constraints	2
1.1	Signal cross-section for $gg \rightarrow h$ with $h \rightarrow W^*W^* \rightarrow l\nu jj$	2
1.2	Main Backgrounds	3
2	Selection using a traditional method	5
2.1	Acceptance and pre-selection requirements	5
2.1.1	Lepton selection	5
2.1.2	Jets selection	6
2.1.3	Missing energy requirement	7
2.2	Selection requirements	8
2.2.1	Di-jet mass requirement	8
2.2.2	Di-jet opening angle	9
2.2.3	Cluster mass M_C	10
2.3	Signal selection efficiency	10
2.4	Background rejection	12
3	Selection using a likelihood method	14
3.1	The Likelihood function	14
3.1.1	Discriminant parameters used	14
3.1.2	Building of the Likelihood function	14
3.2	Likelihood for signal and background events	15
3.3	Results for $m_h = 120 \text{ GeV}/c^2$ to $180 \text{ GeV}/c^2$	16
3.4	Limits on Higgs discovery	17
4	Summary of results	17

1 Cross-sections and physics Constraints

1.1 Signal cross-section for $gg \rightarrow h$ with $h \rightarrow W^*W^* \rightarrow l\nu jj$

The Higgs cross-section production via the gluon-gluon fusion $gg \rightarrow h$ is computed in [1]. Fig. 1.1 shows this cross-section as function of the Higgs mass m_h from 100 GeV to 200 GeV/c at the TeVatron with $\sqrt{s} = 2.0$ TeV. Also shown are the cross-sections \times Branching Ratios in the different channels W^*W^* , Z^*Z^* etc.... The $\sigma \times W^*W^*$ channel turns out to be more than one order of magnitude above the $\sigma \times Z^*Z^*$ predictions. It is therefore a privileged channel to look at for a “low” integrated luminosity of 2 fb^{-1} like in the run II at the TeVatron.

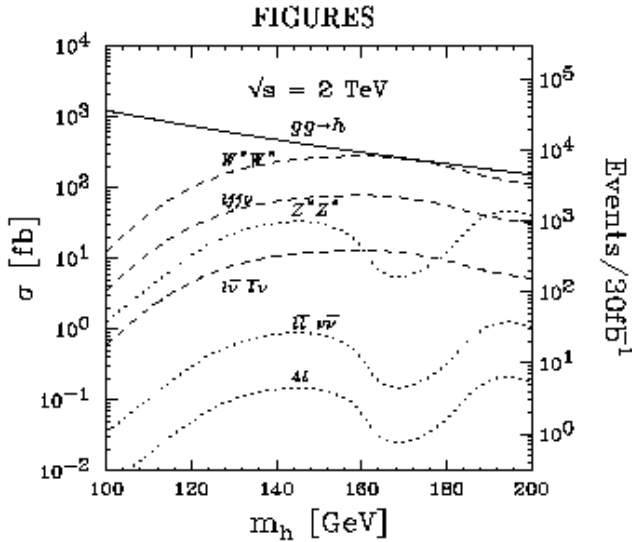


Figure 1.1: Higgs cross-section via the gluon fusion process.

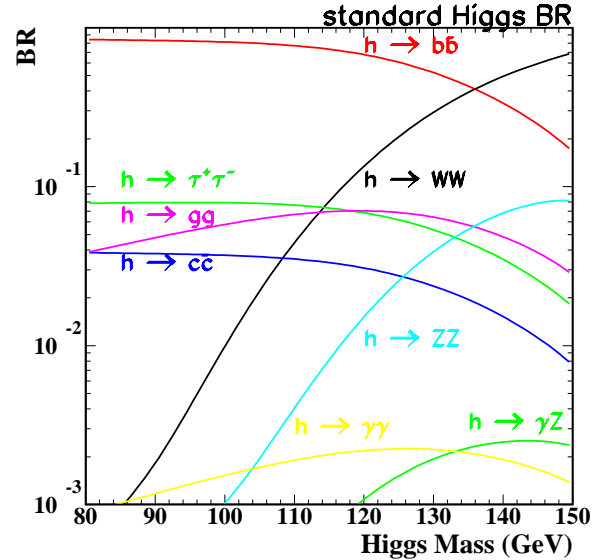


Figure 1.2: Higgs Branching ratios for a standard Higgs

Fig. 1.2 displays the Higgs Branching Ratios in the $[80-150] \text{ GeV}/c^2$ mass range. These results are produced using the HDECAY program [2] in the case of a standard production of the Higgs. As well known, the $h \rightarrow b\bar{b}$ decay is favoured well below the WW^* threshold. For $m_h > 140 \text{ GeV}/c^2$, the $h \rightarrow W^*W^*$ becomes dominant.

Table 1 reports the cross-sections for our specific signal $gg \rightarrow h \rightarrow W^*W^*$. We then require that a W^* decays into 2 leptons while the other decays into two jets. For the leptonic decay of the W^* we restrict our analysis to the electron and muon channels.

Summing the electron and muon channels leads us to a cross-section of about 110 fb for a $m_h = 160 \text{ GeV}/c^2$ Higgs. However, the theoretical cross-section is very sensitive to the Higgs

mass, and favours the real W -pair production. Higgs masses around $m_h = 120 \text{ GeV}/c^2$ are thus expected to be produced with a cross-section below 40 fb.

Higgs Mass (GeV/c^2)	$m_h = 120$	$m_h = 140$	$m_h = 160$	$m_h = 180$
$\sigma(\text{gg} \rightarrow \text{h})$ [fb]	800	480	300	220
$\sigma \times \text{BR}_{\text{WW}}$ [fb]	100	210	300	210
$\sigma \times \text{BR}_{\text{WW}} \times \text{BR}_{\text{l}\nu\text{jj}}$ [fb]	12	15.7	79.6	61.8
Number of events for $\mathcal{L}=10 \text{ fb}^{-1}$	120	157	796	618

Table 1: *Cross-sections \times Branching ratios for our channel $W^*W^* \rightarrow \text{l}\nu \text{ j j}$ where $l = e, \mu$. The numbers, given in fb, are computed for Higgs mass going from 120 GeV/c^2 to 180 GeV/c^2 . The corresponding number of events expected for each of these values are indicated in the last line for an integrated luminosity of 10 fb^{-1} . No cut is applied on these samples.*

1.2 Main Backgrounds

We consider here the backgrounds to our signal characterized by a similar final state:

- the $W + \text{f/g} \rightarrow \text{l}\nu\text{jj}$ events, where a W is produced together with QCD jets. Although their topology is very different than for signal events, a huge cross-section of $\sigma_{W+\text{jets}} \approx 1.34 \text{ nb}$ makes this processus constitute the main background to our signal.

Process	$\sigma(\text{fb})$ 2.0 TeV (PYTHIA)
$W + \text{f/g} \rightarrow \text{l}\nu\text{jj}$	1.3×10^6
$WW \rightarrow \text{l}\nu\text{jj}$	1,348
$t\bar{t} \rightarrow \text{l}\nu\text{jjbb}$	536
$WZ \rightarrow \text{l}\nu\text{jj}$	158

Table 2: *Cross-sections \times Branching ratios for the main backgrounds to our signal. $W^*W^* \rightarrow \text{l}\nu \text{ j j}$ where $l = e, \mu$. These results come from the PYTHIA generator.*

- the $WW \rightarrow \text{l}\nu\text{jj}$ events where W -boson pair decay as our signal. The cross-section of such events is $\sigma_{WW} \approx 1.348 \text{ pb}$ which is a factor ≈ 30 greater than the signal. The only difference with our signal comes from the helicity correlation of the final products [5]. In the Higgs production, both W 's are produced from a spin-0 particle. Both W^+W^- spin correlation and the V-A structure of the W decays result in a distinct topology. This property may be used in the purely leptonic decays of the W 's, for which the opening angle

of the charged lepton is expected to be small in the transverse plane. In our case however, this method would require the identification of the quarks issued from the second W, in order to associate the lepton with its quark counterpart and then compute the angular correlation.

- the $t\bar{t} \rightarrow l\nu jj b\bar{b}$ processus where the final events is characterized by 3 jets with two being b-jets. Here the topology makes these events quite easily distinct from the signal. The cross-section is $\sigma_{t\bar{t}} \approx 536 \text{ fb}$ [3], which is a factor 10 above our signal.
- the $WZ \rightarrow l\nu jj$ events, where the Z decays into two jets and the W decays leptonically. The cross-section for this processus is about $\sigma_{WZ} \approx 158 \text{ fb}$ [3], a factor 3 above the signal.

Table 2 reports all the cross-sections given by [3].

2 Selection using a traditional method

The detection of the signal is based on the selection of a high energy lepton together with two jets (that are not b-quarks jets) and the presence of a quite large missing energy associated to the neutrino.

We use PYTHIA to generate most of the physics processes, interfaced with SHW [4], which provides us with a fast simulation of the effects of the event reconstruction in a typical DØ/CDF detectors.

In the following, all the distributions shown are density probability distributions (distribution normalised to 1.0), except when explicitly specified. These distributions are used to compute a binned-likelihood function devoted to the signal/background discrimination.

2.1 Acceptance and pre-selection requirements

2.1.1 Lepton selection

The lepton acceptance is defined to be in the pseudo-rapidity range $|\eta_l| < 2.0$. Only electrons or muons with $p_T > 15 \text{ GeV}/c$ are kept.

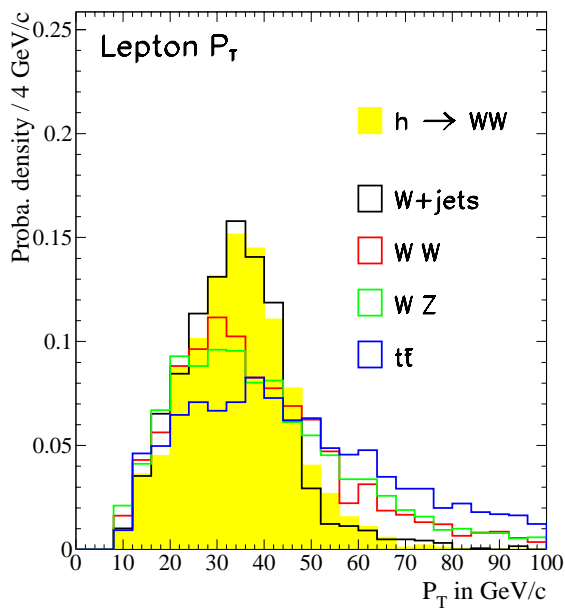


Figure 2.3: *Lepton p_T distribution for signal and backgrounds. These distributions are computed for a $m_h = 160 \text{ GeV}/c^2$ Higgs.*

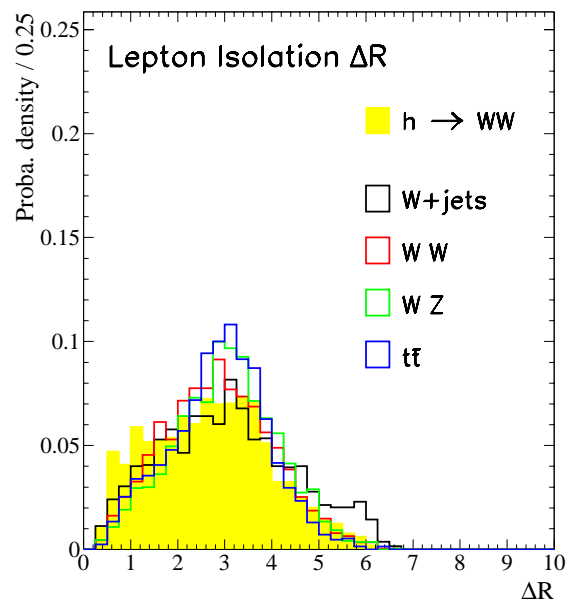


Figure 2.4: *Isolation of the lepton for signal and backgrounds. These distributions are computed for a $m_h = 160 \text{ GeV}/c^2$ Higgs.*

Electrons are selected with an EM fraction such that $E_{\text{had}}/E_{\text{EM}} \leq 0.125$ and an associated track within a 30° cone around the EM deposition. The lepton isolation requires that any jet around the lepton to be outside a cone defined by $\Delta R(j, l) > 0.3$ in the $(\Delta\phi, \Delta\eta)$ plane. Fig. 2.3 and 2.4 display the p_T lepton spectrum and the $\Delta R(j, l)$ for the signal and all the backgrounds.

2.1.2 Jets selection

A. Jet acceptance

The jet acceptance is defined to be in the pseudo-rapidity range $|\eta_j| < 1.0$ to reduce the selection of W+jets events. Those events indeed have soft QCD jets, pointing most of the case in the towards the end-cap.

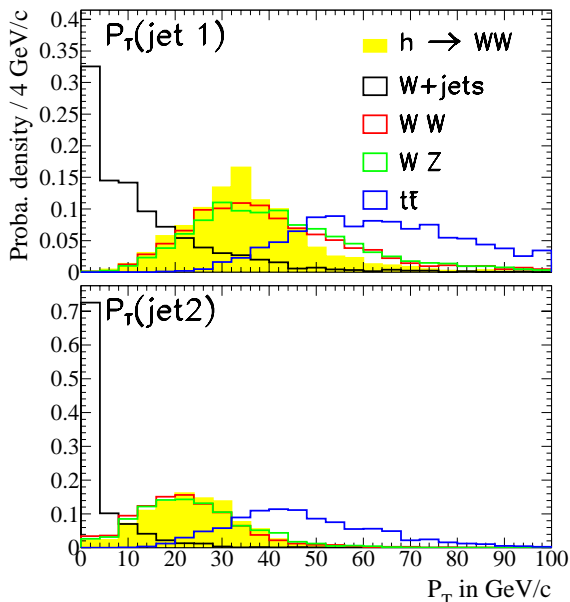


Figure 2.5: Jets p_T distribution for signal and backgrounds. These distributions are computed for a $m_h = 160 \text{ GeV}/c^2$ Higgs.

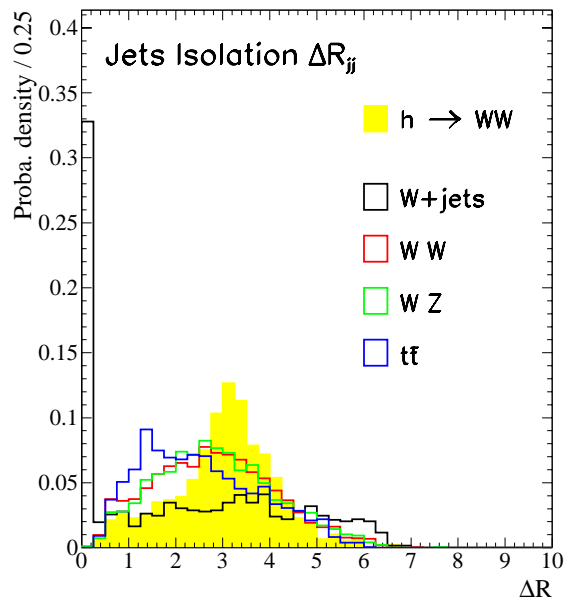


Figure 2.6: Isolation of the jets for signal and backgrounds. These distributions are computed for a $m_h = 160 \text{ GeV}/c^2$ Higgs.

Jets are required to have a 5 GeV deposit in the calorimeters, and tracks associated within a cone of 30° around the cluster. the selection requires the presence of two jets above 15 GeV/c in p_T , and well isolated with $\Delta R(j, j) > 0.7$. This last requirement allows us to reject the selection of soft QCD jets present in the W+jets events. Fig. 2.5 displays the jet 1 and 2 p_T for the signal compared to backgrounds. We clearly see that the requirement reduces the selection of W+jet

events. Fig. 2.6 shows the isolation between the two jets before the cut. Again a good rejection is obtained against W +jet events and $t\bar{t} \rightarrow \nu jj b\bar{b}$ events, where more than two jets can be seen.

B. Extra jet veto

In order to reduce the background due to $t\bar{t} \rightarrow \nu jj b\bar{b}$ events, we require at this stage that no event with a third jet above $p_T > 25$ GeV/c is selected. The sensitivity to this cut has been investigated. Lower values for this upper bound leads to drastic loss in signal events selection. Fig. 2.7 shows the p_T distribution for a third jet in signal and background events. A cut below 10-15 GeV removes more than 60% of the signal events...

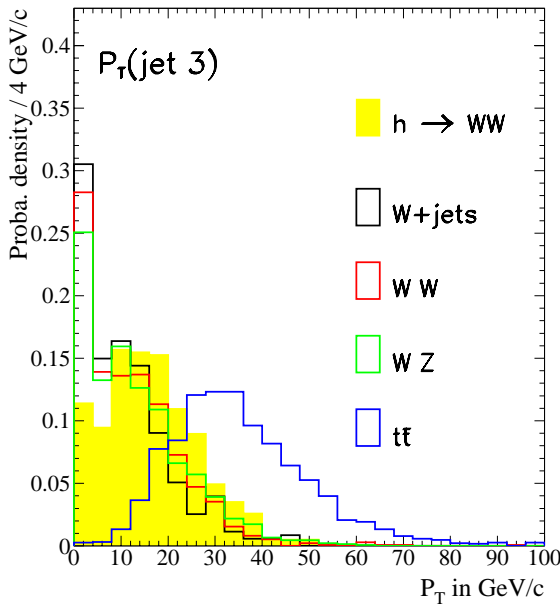


Figure 2.7: *Third jets p_T distribution for signal and backgrounds. These distributions are computed for a $m_h = 160$ GeV/c² Higgs.*

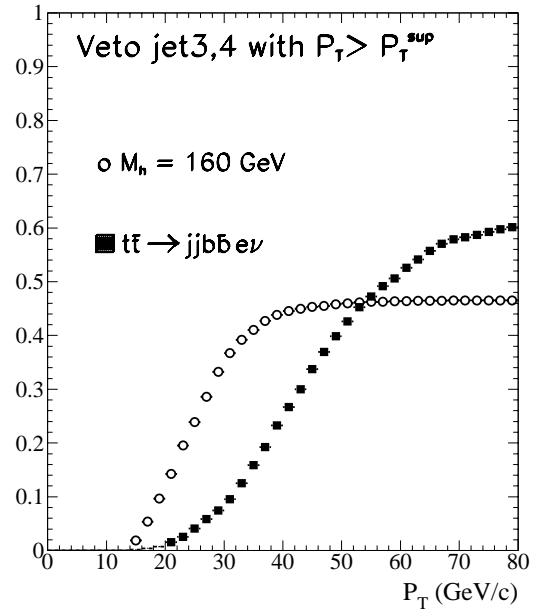


Figure 2.8: *Sensitivity to the extra jet veto applied on jet 3 and 4 if any, for signal and the $t\bar{t} \rightarrow \nu jj b\bar{b}$ background.*

The sensitivity to the jet-veto cut for any jet 3 and 4 is displayed in Fig. 2.8 as function of the jet energy threshold. A cut at 25 GeV/c removes efficiently $t\bar{t} \rightarrow \nu jj b\bar{b}$ background events while preserving more than 80% of the remaining signal.

2.1.3 Missing energy requirement

We require a threshold on the total missing (transverse) energy of $E_T > 15$ GeV/c. This allows us to select at least one leptonic W -boson decay with a neutrino.

Fig. 2.9 shows the missing transverse energy before the cut is applied for signal and all the different backgrounds. The distributions show some significant difference in the case of $t\bar{t} \rightarrow l\nu jjb\bar{b}$ and WZ events. In the first case, the two W's can indeed decay in $l + \nu$ channel. Fig. 2.10 displays the variation of the missing energy distribution for different generated Higgs mass. When the Higgs decay into two off-shell W's, the E_T spectrum tends to peak at lower values, as expected. In these cases, this results in a degradation of the discrimination from backgrounds. For lower Higgs mass values, this cut is reduced to $E_T > 10$ GeV/c.

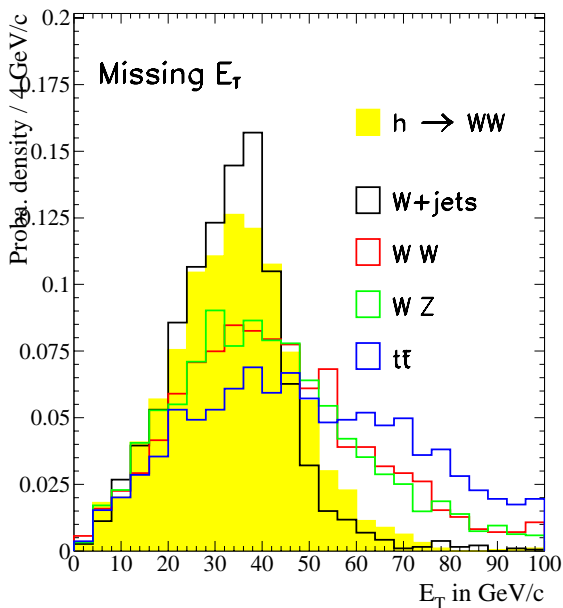


Figure 2.9: *Missing transverse energy distribution for signal and backgrounds. These distributions are computed for a $m_h = 160$ GeV/c² Higgs.*

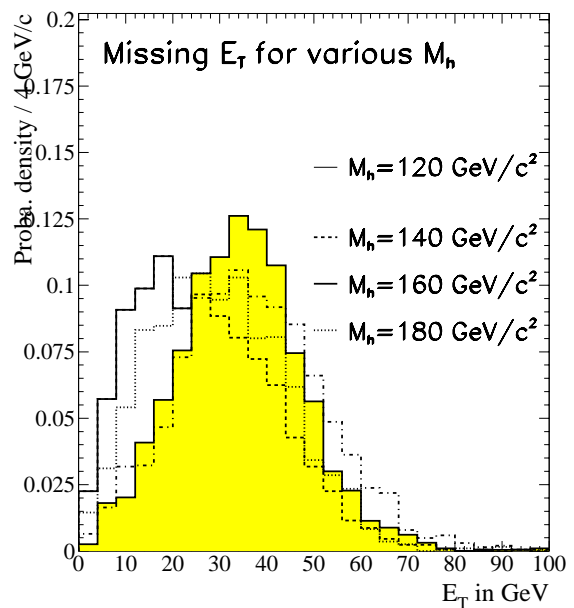


Figure 2.10: *Missing transverse energy distribution for different Higgs mass going from 120 to 180 GeV/c².*

2.2 Selection requirements

The selection is based on the cuts presented so far, to which we add the following requirements.

2.2.1 Di-jet mass requirement

The di-jet mass $M(j_1, j_2)$, where we keep the combination giving the highest mass, is represented in Fig. 2.11 for signal and background, and in Fig. 2.12 for different Higgs mass samples. It appears clearly that the $t\bar{t} \rightarrow l\nu jjb\bar{b}$ background is peaked at higher reconstructed masses, as expected for b-jets events. Mass spectrum also concentrate to the lower values for the QCD jets

of the W +jets events. At the same time, the distributions show a relative stability for signal events for Higgs masses ranging between 140 and 180 GeV/c^2 .

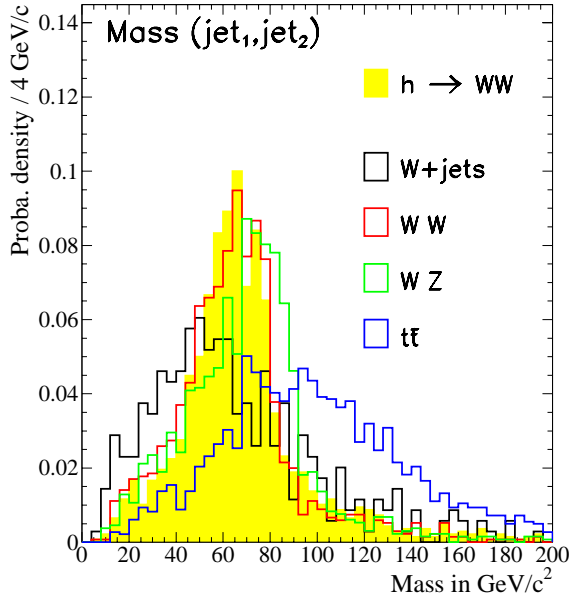


Figure 2.11: *Dijet Mass distribution for signal and backgrounds. These distributions are computed for a $m_h = 160 \text{ GeV}/c^2$ Higgs.*

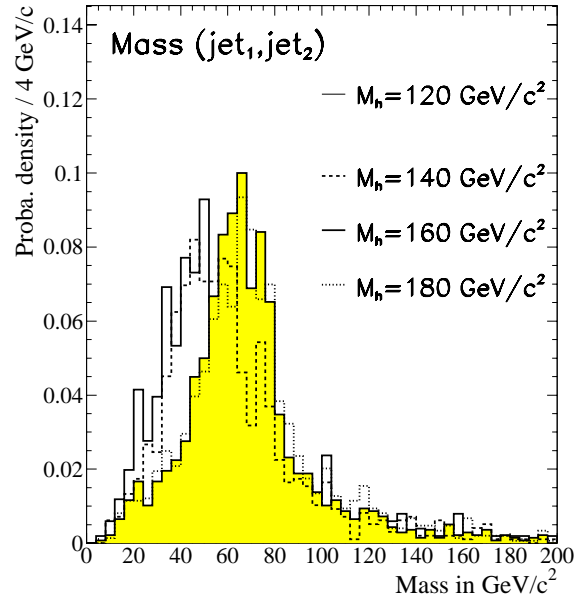


Figure 2.12: *Dijet Mass distribution for Higgs with mass going from 120 to 180 GeV/c^2 . The jets combination giving the highest mass is kept.*

2.2.2 Di-jet opening angle

Fig. 2.13 displays the opening angle of the jets for the signal and backgrounds in the transverse plane. The angle is expected to be higher for the signal events, whereas a flat distribution is observed for all backgrounds.

Fig. 2.14 gives this distributions for all Higgs masses. It shows that off-shell W 's productions tend to have a flatter distribution than for a 160 GeV/c^2 Higgs.

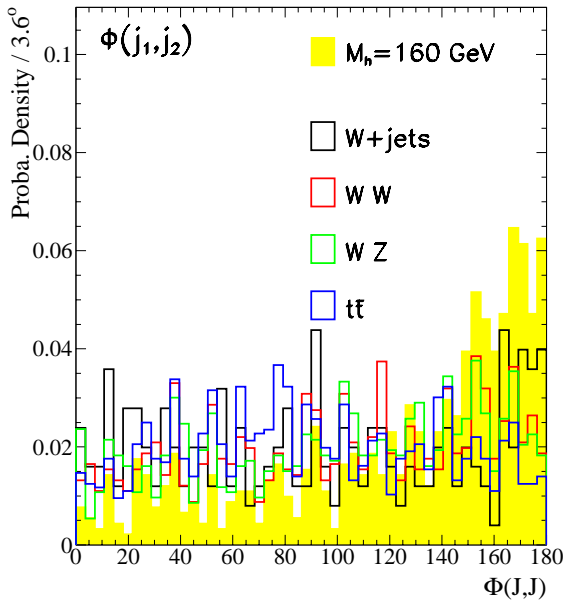


Figure 2.13: *Dijet opening angle distribution for signal and backgrounds. These distributions are computed for a $m_h = 160 \text{ GeV}/c^2$ Higgs.*

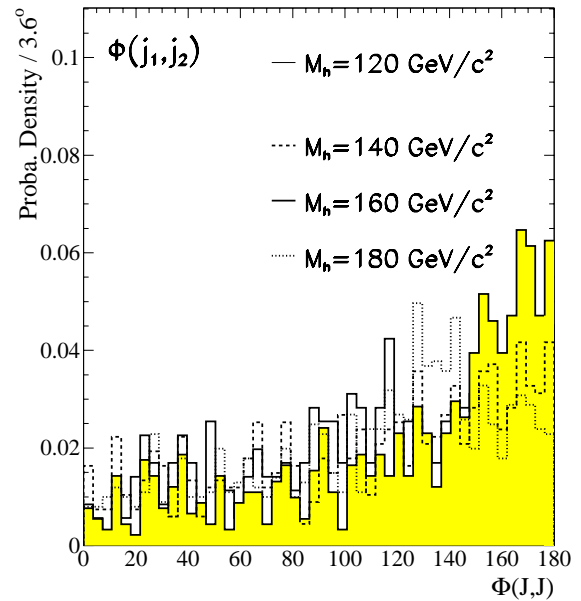


Figure 2.14: *Dijet opening angle distribution for Higgs with mass going from 120 to 180 GeV/c^2 . The jets combination giving the highest mass is kept.*

2.2.3 Cluster mass M_C

This latter is defined in [1] by:

$$M_C = \sqrt{p_T^2(lj) + m^2(jj) + \cancel{E}_T}$$

where the transverse mass of the (lepton, jet, jet) system is used together with the transverse missing energy to form the mass cluster, corresponding roughly to the Higgs mass. This variable is represented in Fig. 2.15 for signal and background events, and in Fig. 2.16 for different generated Higgs mass samples. These figures show a good discriminating power against most of the backgrounds, in particular $t\bar{t} \rightarrow l\nu jj b\bar{b}$ and WW and WZ events.

2.3 Signal selection efficiency

Table 3 reports the results of the acceptance and selection cuts on signal events. No likelihood cut is applied at that stage. Sample of 10,000 events are used to estimate the efficiency for W's on-shell.

Efficiency is found to be 13.6% for $m_h = 160 \text{ GeV}/c^2$. For lower Higgs masses, efficiencies

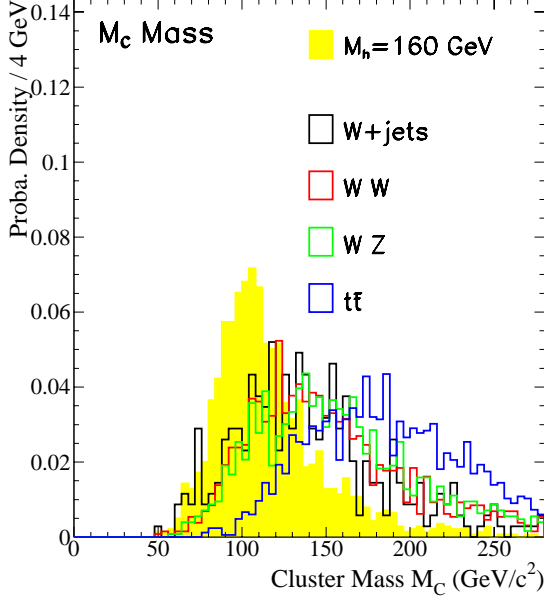


Figure 2.15: Cluster Mass distribution for signal and backgrounds.

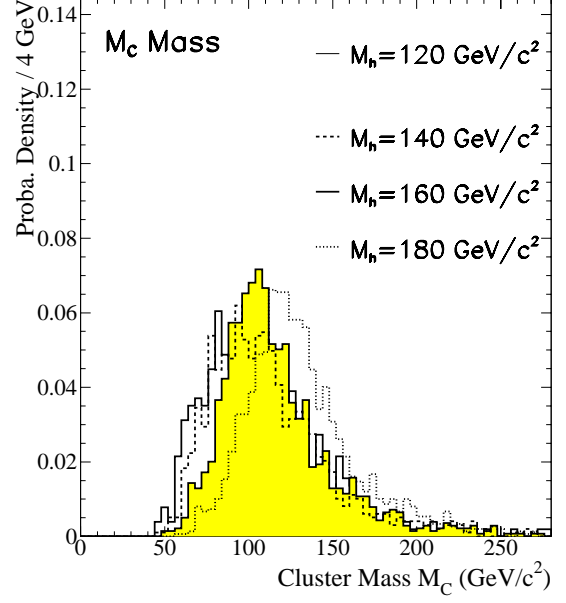


Figure 2.16: Cluster Mass distribution for Higgs mass going from 120 to 180 GeV/c^2 .

M_h (GeV/c^2)	120	140	160	180
Initial # events	3,000	3,000	10,000	3,000
Reconstruction	1,730	1,924	6,440	2,015
Lepton (p_T , η , ΔR)	1,455	1,758	6,162	1,955
Jets: (p_T and η , ΔR)	371	613	2,726	906
Missing Energy cut	248	510	2,557	831
Jet Veto Cut	230	443	2,074	674
Pre-selection (%)	$8.3 \pm 0.5\%$	$14.8 \pm 0.6\%$	$20.7 \pm 0.4\%$	$22.5 \pm 0.8\%$
$40 < M(j,j) < 110$	98	234	1,522	488
$140^0 < \Phi(j,j)$	98	234	1,520	487
$40 < M_C < M_h + 10 \text{ GeV}$	82	184	1,365	336
Full Selection (%)	$2.7 \pm 0.3\%$	$6.1 \pm 0.4\%$	$13.6 \pm 0.3\%$	$11.2 \pm 0.6\%$

Table 3: Pre-selection efficiency for the signal events generated for four different Higgs masses

are degraded because W 's are not produced off-shell, which result in a lowering of the average lepton and jet p_T , and therefore in a lower pre-selection efficiency. For $m_h = 180 \text{ GeV}/c^2$, the loss in efficiency is due to the increase in the reconstructed cluster mass (and di-jet) as seen in Fig. 2.16, because of extra jet-momentum.

2.4 Background rejection

Table 3 reports the results of the acceptance and pre-selection cuts on background events. High rejections are obtained for the main backgrounds in term of selection efficiency.

Backgrounds	W+jets	WW $\rightarrow l\nu jj$	WZ $\rightarrow l\nu jj$	$t\bar{t} \rightarrow l\nu jj b\bar{b}$
Pre-selection (%)	$1.36 \pm 0.04\%$	$17.8 \pm 0.4\%$	$15.0 \pm 0.6\%$	$9.7 \pm 0.3\%$
Full Selection (%)	$0.30 \pm 0.02\%$	$5.5 \pm 0.2\%$	$3.7 \pm 0.3\%$	$0.8 \pm 0.1\%$

- WW $\rightarrow l\nu jj$ and WZ $\rightarrow l\nu jj$ events: these backgrounds are pre-selected with efficiencies comparable to the one obtained for the signal. These events have comparable shapes to the signal and are very difficult to discriminate from Higgs signal. However, some differences are seen in the opening angle between the jets.
- $t\bar{t} \rightarrow l\nu jj b\bar{b}$ events are rejected in the pre-selection mostly by the jet veto requirement. The cluster mass and dijet mass reconstructed tend also to be higher than the one reconstructed for our signal.
- W + f/g $\rightarrow l\nu jj$ events have a different topology than Higgs events. They are thus well rejected at the 3/1,000 level. The most efficient requirements are the jet-acceptance cut and the jet p_T cuts. The dijet mass cut, as well as the dijet opening angle also bring a factor 5 on already pre-selected events. However, given the cross-section of this background, the 3/1,000 factor still appears insufficient.

The estimation of the efficiency in the background rejection is given by the luminosity needed to ensure a 3σ or 5σ significance discovery. Table 4 reports the ratio S/\sqrt{B} for all individual backgrounds to the $m_h = 160 \text{ GeV}/c^2$ signal samples (first line) computed for an integrated luminosity of 1 fb^{-1} . The luminosity needed to get a 3σ or a 5σ significance is indicated in line 2. If one sums over all the backgrounds, the ratio S/\sqrt{B} is given by:

$$\frac{S}{\sqrt{B}} = \sqrt{\mathcal{L}} \times \frac{\sigma_S \times \epsilon_S}{\sqrt{\sigma_{\text{wjet}} \times \epsilon_{\text{wjet}} + \sigma_{\text{WW}} \times \epsilon_{\text{WW}} + \sigma_{\text{WZ}} \times \epsilon_{\text{WZ}} + \sigma_{t\bar{t}} \times \epsilon_{t\bar{t}}}} = \sqrt{\mathcal{L}} \times 0.117$$

Backgrounds	W+jets	WW \rightarrow $l\nu jj$	WZ \rightarrow $l\nu jj$	tt \rightarrow $l\nu jjbb$
S/ \sqrt{B} per fb $^{-1}$	0.12	0.89	3.16	3.69
\mathcal{L} for 3 σ in fb $^{-1}$	610	11.2	0.9	0.7

Table 4: *1st line: Ratio S/ \sqrt{B} for a $m_h = 160$ GeV/ c^2 higgs and the four main background, computed for a luminosity of 1 fb $^{-1}$. Both electron and muon channel are considered. Line 2: Needed luminosity to reach a 3 σ significance discovery for each individual backgrounds. No likelihood cut is applied at that stage.*

and the luminosity needed for a 3 σ discovery (no likelihood cut used) therefore is $\mathcal{L} = 660$ fb $^{-1}$!!

This shows that the main constraint comes from the W+jets background, because of its huge cross-section in ppbar collision. In order to improve our discrimination, we therefore need to apply further cuts. We choose to use a likelihood cut, described, in the next section.

3 Selection using a likelihood method

The traditional method does not bring enough rejection in background events (mainly the $W+f/g \rightarrow l\nu jj$ events) because it does not fully take into account the differences in the topology between signal and background events. We choose here to apply the likelihood technique, based on all the variable distributions presented in the previous section. This technique is explained in details in [6].

3.1 The Likelihood function

The likelihood function is based on the density probability functions of the parameters used, computed for all backgrounds and signal. We first define the set of parameters used, and then present the likelihood definition.

3.1.1 Discriminant parameters used

Here is the set of variables we use to build this likelihood function:

1. Jet 1,2 variables: $p_T^{j1}, p_T^{j2}, \Delta R_{jj} \Rightarrow v_1, v_2, v_3$
2. Lepton variable: $P_T^l \Rightarrow v_4$
3. Missing energy : $E_T^{\cancel{e}} \Rightarrow v_5$
4. Jet opening angle: $\Delta\Phi(j,j) \Rightarrow v_6$
5. Jet 3/4 : $P_T^{j3} \Rightarrow v_7$
6. Jet-jet Mass : $M(j_1, j_2) \Rightarrow v_8$
7. Cluster Mass : $M_C \Rightarrow v_9$

3.1.2 Building of the Likelihood function

The likelihood method is explained in detail in [6]. After defining the discriminant variables, the method is based on the MC probability density functions observed for signal and all different background events. Given an event, we then compute the probability using each variables that the event is a signal or a background event. The total probability for the event to be a signal event for the variable v_i is then given by:

$$p_{v_i}^S(x_i) = \frac{v_i^S(x_i)}{\sum_{j=S,B} v_i^j(x_i)}$$

where $v_i^{S/B}(x_i)$ is the probability density function to be a signal (S) or a background (B) associated to the variable v_i . We then compute the likelihood for these event to be signal using all discriminant variables \vec{x} :

$$\mathcal{L}(\vec{x}) = \frac{\prod_{i=1}^n p_i^S(x_i)}{\sum_{j=S,B} \prod_{i=1}^n p_i^j(x_i)}$$

3.2 Likelihood for signal and background events

Fig. 3.17 shows the likelihood normalised to one for the signal and all four backgrounds on an extended scale. The signal is clearly concentrated in higher likelihood bins. W+jets events appear peaked in the first bins, with about less than 1/1,000 events with a likelihood above 0.7. WW and WZ events being topologically more similar to our signal go to higher likelihood values up to 1.0. This constitutes an irreducible background as long as no identification of the fermion flavour is performed.

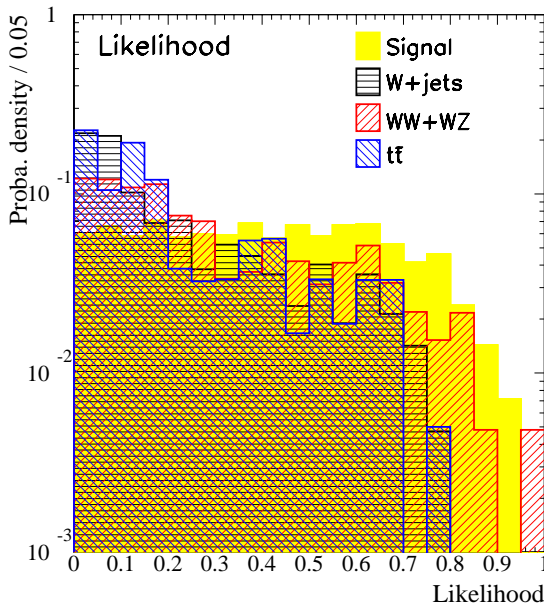


Figure 3.17: *Likelihood for signal and backgrounds. All the selection cuts are applied.*

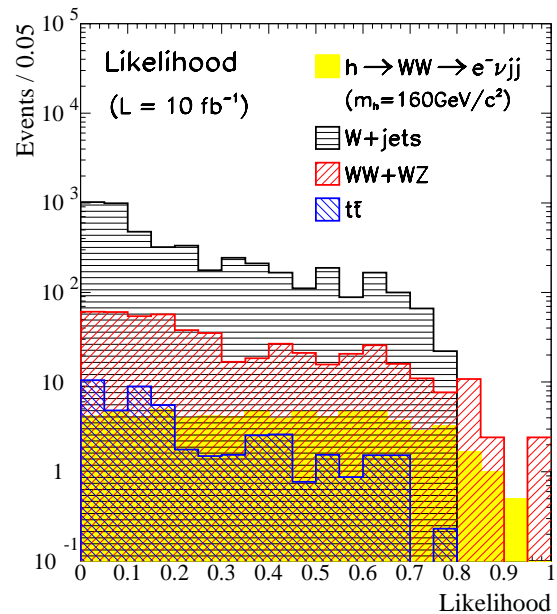


Figure 3.18: *Likelihood in number of events for signal and backgrounds. All cuts are applied*

Fig. 3.18 displays the events likelihood in event numbers for an integrated luminosity of 10 fb^{-1} after normalising properly by the production cross-sections. It turns out that the likelihood cut must be set above 0.80 to avoid the selection of W+jets events which constitute the most lethal background. We haven't use the distinction between WW and

our signal’s topology provided by the angular W decay’s products correlations. With this likelihood function, the presence of a SM Higgs may only be seen as an extra number of events over the WW distributions. Table 5 reports the cross-sections for a $m_h = 160 \text{ GeV}/c^2$ Higgs and the total background. This latter is composed by the $WW \rightarrow l\nu jj$ events for likelihood above 0.8.

Cross-section (in fb^{-1})	Higgs ($m_h = 160 \text{ GeV}/c^2$)	Backgrounds				
		W+jets	WW	WZ	$t\bar{t}$	TOTAL
Likelihood Cut						
L > 0.80	0.32 ± 0.03	—	1.75	—	—	1.75 ± 1.7
L > 0.85	0.15 ± 0.01	—	0.54	—	—	0.54 ± 0.05
L > 0.90	0.06 ± 0.01	—	0.27	—	—	0.27 ± 0.03

Table 5: *Expected cross-section (in fb^{-1}) for signal and background event after the application of the likelihood cut. The uncertainties are quoted assuming a 10% error in the evaluation of the efficiency.*

For a likelihood $L > 0.80$, the ratio $S/\sqrt{B} = 0.242 \times \sqrt{\mathcal{L}}$. A 3σ significance therefore requires a luminosity of $\mathcal{L} = 150 \text{ fb}^{-1}$, while a 2σ significance exclusion needs $\mathcal{L} = 65 \text{ fb}^{-1}$.

3.3 Results for $m_h = 120 \text{ GeV}/c^2$ to $180 \text{ GeV}/c^2$

The analysis is optimised for a $160 \text{ GeV}/c^2$ Higgs and shows a decrease in the performance for off-shell W decays, as seen in the selection efficiencies. Table 6 report the cross-sections expected for signal and backgrounds for a likelihood greater than 0.80. As expected, the sensitivity to the signal is degraded: below the W threshold, the topology changes become significant (lepton and missing energy) and lead to a decrease in the discrimination against the W+jet background. Above the W threshold, the Cluster Mass and jet invariant masses distributions are changed such that the $t\bar{t}$ background become more important.

M_h	120 GeV	140 GeV	180 GeV
Signal (fb)	0.12 ± 0.01	0.30 ± 0.03	0.39 ± 0.04
Background (fb)	1.96 ± 0.20	1.80 ± 0.20	3.18 ± 0.32

Table 6: *Expected cross-section (in fb^{-1}) for signal and background event after the application of the likelihood cut. The uncertainties are quoted assuming a 10% error in the evaluation of the efficiency.*

3.4 Limits on Higgs discovery

Figure 3.19 shows the ratio S/\sqrt{B} as a function of the integrated luminosity for $m_h = 160 \text{ GeV}/c^2$. It turns out that a 3σ significance discovery in this channel alone requires an integrated luminosity above 160 fb^{-1} . However, it seems that a 2σ significance (for 95% CL exclusion) may be reached with 2 experiments accumulating 30 fb^{-1} each.

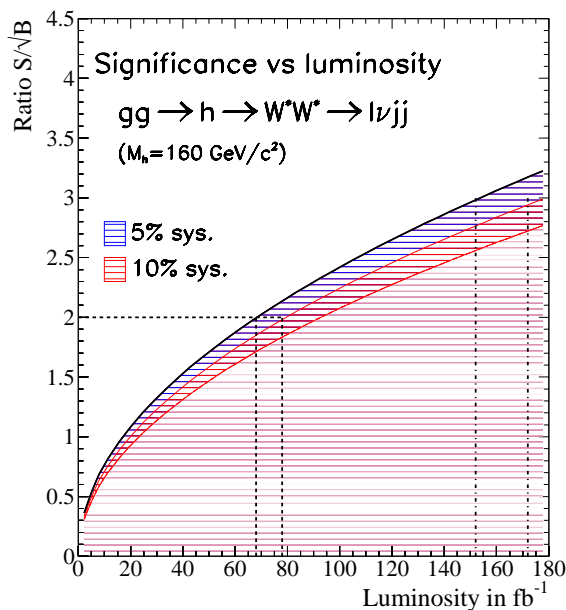


Figure 3.19: *Significance as function of the luminosity for a Higgs mass signal of 160 GeV. Shown are the effects of a 5% and 10% systematics on the efficiency+background estimations.*

4 Summary of results

In this note, we investigate the potentiality of a SM Higgs discovery in the $gg \rightarrow h$ with $h \rightarrow W^*W^* \rightarrow lvjj$ channel at the TeVatron run II. In this channel, the main background comes from the W +jets events, produced in the $ppbar$ collisions with a cross-section 25,000 times our signal cross-section. This background is reduced to a negligible level by using a combination of pre-selection and selection cuts, together with a likelihood method. The other important background comes from the W -pair production, which appear irreducible if one does not use the angular correlation between the lepton and the quark issued from the W^+W^- decays of the Higgs (spin 0).

Monte Carlo studies show that a 3σ significance effect needs an integrated luminosity of 150 fb^{-1} , whereas a 95% CL exclusion requires a luminosity of about 60 fb^{-1} , for a $160 \text{ GeV}/c^2$ Higgs. We conclude that this channel has to be used in combination with the associated Higgs production channel.

References

- [1] “Extended the Higgs Boson Reach at Upgraded TeVatron”, Tao Han and Re-Jie Zhang, HEP-PH/9807424
- [2] **HDECAY** program by M. Spira et al., <http://home.cern.ch/m/mspira/www/>
- [3] PYTHIA program
- [4] Simulation Package for Run II SUSY/Higgs Workshop.
<http://www.physics.rutgers.edu/~jconway/soft/shw/shw.html>
- [5] M. Dittmar “Searching for the Higgs and other exotic object”, Lectures given at the 30eme Ecole d’Ete de Physique des Particules, Marseilles 7-11 september 1998.
- [6] “Search for the standard Model Higgs Boson in e+e- collisions at 161-172 GeV” , CERN 97-115.